

Boundary Effects in Planar Networks: Pentagons Dominate Marginal Cells

Kai Xu^{1,*}, Fei He²

¹ Fisheries College, Jimei University, Xiamen, 361021, China

² School of Mathematical Sciences, Xiamen University, Xiamen, 361005, China

Contact author: kaixu@jmu.edu.cn, kxu2013@gmail.com

Abstract—The topological and geometrical features in the boundary zone of planar polygonal networks remain poorly understood. Based on observation and mathematical proof, we propose that the average edge number of marginal cells in *Pyropia haitanensis* thalli, a two-dimensional (2D) biological polygonal network, is exactly five. We demonstrated that this number is maintained by specific division patterns. Furthermore, we identified profound limitations of Lewis's law and Aboav-Weaire's law by comparing the topological and geometrical parameters of marginal cells and inner cells. Strong boundary effects were manifested in the distributions of interior angles and edge lengths of marginal cells. Similar to inner cells, cell division tended to occur in marginal cells with large sizes. Our findings suggest that inner cells should be strictly defined based to their positional relationship to the marginal cells.

Introduction—The topological and geometrical features of two-dimensional (2D) trivalent polygonal networks have been extensively studied over the past several decades ^[1]. Analyzing the evolutionary dynamics of 2D polygonal network not only help uncover the fundamental laws of nature but also provides new insights into the biophysical and biomathematical mechanisms underlying life phenomena. Two empirical laws, Lewis's law and Aboav-Weaire's law, have been widely used to describe the relationships between cell size, edge number, and spatial arrangement in 2D planar tiling ^[1, 2]. These laws have been validated across various 2D polygonal networks, ranging from atomic to cosmic scales ^[3, 4].

To the best of our knowledge, previous studies have primarily focused on the inner regions of such network, where all examined polygonal cells are fully surrounded by neighboring cells. However, certain 2D biological networks, such as the thallus of *P. haitanensis*—composed of a monolayer of polyhedral cells—exhibit a smooth boundary. In these networks, one edge of each marginal cell is not shared with any other cell, and the coordination number of every vertex is strictly equals to three. Intuitively, the marginal cells display distinct topological and geometrical features compared to inner cells.

To address this gap, we quantified the edge number, size, edge length, interior angle and neighboring relationship of marginal cells in *P. haitanensis*. Additionally, we analyzed the relationship

between cell division and cell shape parameters. Our findings provide valuable insights that may be applicable to a wide range of scientific and practical contexts.

Methods—The software Amscope Toupview 3.0 was used to analyze the topological and geometrical parameters of cells from the *P. haitanensis* strain Sansha, as well as red and green mutant cells from the strain WO. In this study [Fig. 1(a)], we define marginal cells (MCs) as those located at the boundary of the polygonal cell network. Neighboring cells of MCs (NC-MCs) are characterized by their adjacency to MCs, sharing at least one common edge. Inner cells (ICs) are fully enclosed within the network, with no direct connection to NC-MCs. Each marginal cell contains a marginal edge (ME), positioned at the tissue boundary and belonging exclusively to the marginal cell. Additionally, each marginal cell contains two marginal angles (MA), which are directly associated with the ME [Fig. 1(a)].

For each polygonal cell, we counted the number of edges (n), and measured the area (A_C), perimeter (P), edge length, interior angles, and the coordinates of the center (X_{PC} , Y_{PC}) and vertices (X_V , Y_V). We used software R (version 4.0.0) with package Conicfit (version 1.0.4) to fit an ellipse based on the coordinates of the vertices of each polygonal cell [5]. The area of the ellipse's maximal inscribed polygon (A_{EMIP}) is given by $A_{EMIP} = 0.5nabsin(2\pi/n)$, where n is the number of edges of inscribed polygon, a is the semi-major axis, b is the semi-minor axis [6].

The effects of cell division on topological and geometrical parameters were identified through time-series observation. The size ratio of daughter cells was calculated as $SR = A_S \div A_L$, where A_S and A_L are area of the smaller and larger daughter cells, respectively. To quantify the relative position of the paired edges in the mother cell that are transected by cell divisions, the number of interval edges between the paired sides was counted in opposite directions, and the smaller number was used in this study [7].

Edge number distribution—Lewis first reported two significant and conserved features of the edge number distribution in trivalent 2D polygonal network: the average edge number \bar{n} is six and the hexagon predominant [8, 9]. Here, we found that inner cells (ICs) have an average edge number \bar{n}_{ICs} of approximately six [Tab. S1] and are predominantly hexagons [Fig. 1(b)]. In contrast, marginal cells (MCs) have an average edge number \bar{n}_{MCs} of approximately five and are predominantly pentagons. For inner cells, $\bar{n}_{ICs} = 6$ can be derived from Euler's 2D equation under two conditions: every three edges meet at a vertex, and the number of polygonal cells is sufficiently large [1]. Based on our results, we propose that previous studies reporting $\bar{n} = 6$ for trivalent 2D network may have focused exclusively on ICs. These findings are consistent with our earlier study [7], which found that \bar{n} increases from four to six as the number of cells in *P. haitanensis* thalli increase from five to a large number. We suggest that the variation in \bar{n} is closely associated to the proportion of MCs. Furthermore, $\bar{n}_{MCs} = 5$ for the marginal cells could be considered as a specific case of the inner cells. Below we provide two

simple mathematical proofs [Fig. 1(c)].

First method: Suppose the cells are very small relative to the boundary of the polygonal network, we can assume that the boundary is locally a straight line. By joining the polygonal network with its mirror image across the boundary and translating the mirror image a little to ensure that the coordinate number equals three, this construction results in a polygonal network without boundary. In this case, each marginal cell can be considered as an inner cell. Suppose the edge number of a marginal cell is n_{MC} , then after translation the new cell has an edge number of $n_{MC} + 1$. Thus, on average sense, we should have $\bar{n}_{MCs} + 1 = \bar{n}_{ICs} = 6$, hence $\bar{n}_{MCs} = 5$. Second method: We assume that the edges intersect the boundary perpendicularly. By joining the polygonal network with its mirror image across the boundary and then erasing the boundary edges, then each marginal cell is doubled into an inner cell. After doubling the new cell has an edge number of $2(n_{MC} - 1) - 2$. Thus, we have $2(\bar{n}_{MCs} - 1) - 2 = \bar{n}_{ICs} = 6$, hence $\bar{n}_{MCs} = 5$.

Lewis's law and Aboav-Weaire's law—Lewis also observed that the area of an n -edged cell increases linearly with n [9]. This relationship, known as Lewis's law, is considered as a conserved (though empirical) law in trivalent 2D network [1]. In this study, for each strain or mutant, the area A_C of all three kinds of cells were increased with n [Fig. 1(d)]. However, the average value of A_C of MCs, NC-MCs, and ICs were very similar [Tab. S1]. A similar trend was observed for cell perimeter P [Fig. 1(e), Tab. S1]. These results suggest that cells of different size tend to distribute uniformly within the 2D polygonal network. Given the significant difference in \bar{n} between MCs and ICs, Lewis's law appears to hold locally but not globally.

Aboav-Weaire's law, another empirical law, states that the many-edged cell tend to neighbor with few-edged cells, and vice versa [10, 11]. In this study, the average edge number (m) of neighboring cells for all three cell types decreased as n increased [Fig. 1(f)]. Additionally, according to Aboav-Weaire's law, m for NC-MCs should decrease due to their adjacency to MCs. This hypothesis was confirmed, as the average m for NC-MCs was generally lower than that for ICs [Tab. S1]. Thus, Aboav-Weaire's law also appears to hold only locally.

Ellipse packing—Previous studies have suggested that polygonal cells in trivalent 2D networks tend to form the ellipse's maximal inscribed polygon (EMIP), a phenomenon termed Ellipse packing [7, 12, 13]. This study found that the area A_C of all cell types is approximately 0.85 times the area of the EMIP (A_{EMIP}) [Tab. S1]. This suggests that maintaining an optimal cell size may be more important for the cells (including MCs) than adhering to Lewis's law.

Due to the restrictions of Ellipse Packing and $\bar{n}_{ICs} = 6$, the interior angles of ICs peaked in the range of 110–130° [Fig. 2(a)]. Theoretically, $\bar{n}_{MCs} = 5$ should cause the angle distribution of MCs to peak around 108°. However, about 42% of the interior angles of MCs fell within 80–100°, primarily due

to the fact that about 80% of the marginal angles (MAs), which accounting for roughly 40% of the interior angles, were in range of 80–100°. In addition, the distribution of edge lengths showed obvious differences between MCs and ICs [Fig. 2(b)], which mainly due to their similar mean perimeters but different average edge number [Tab. S1]. Similarly, the edge length distribution was influenced by the marginal edges (MEs), which accounting for about 20% of MC edges. These results indicate strong boundary effects on the distributions of angles and edge lengths in MCs.

Cell division—The division of an inner cell increases the cell number by one and the edge number by six, making $\bar{n}_{ICs} = 6$ a topological consequence of cell division in biological trivalent 2D networks [8, 9]. Previous studies suggest that mitotic division of *Drosophila* epithelia tends to occur in large cells which approximately contains one more edge compared with resting cells [16, 17]. Here, we found that, regardless cell positions or strains (and/or mutants), the mean A_C of dividing cells was at least 30% higher than that of resting cells [Fig. 3(a)], while the mean P of the dividing cells was 14~20% higher [Fig. 3(b)]. The mean n of dividing cells was 6~10% higher than that of resting cells, while difference in aspect ratio a/b and m were less than 5% [Fig. 3(c)]. These findings, along with previous studies [16, 17], suggest that cell size is a better indicator of dividing cells than n , a/b , and m .

In general, mitosis tends to divide a cell equally, as verified by a previous study on ICs of *P. haitanensis* thalli [7] and confirmed in this study for MCs [Fig. S1(a)]. In addition, due to $\bar{n}_{MCs} = 5$, 96% of the number of interval edges were one [Fig. S2(b)]. The division of an MC that transects the ME produces two daughter MCs; otherwise, it produces only one daughter MC [Fig. S1(c)]. Based on the percentages of five types of division observed in MCs and \bar{n} of dividing MCs was 5.16 [Fig. 3(c)], we found that the daughter MCs maintained an average edge number of 5.06. Therefore, $\bar{n}_{MCs} = 5$ is also a topological consequence of specific patterns of cell division. Further studies are needed to explore the underlying mechanisms of the division patterns. Markov chain models have also validated that the predominance of hexagons in epithelia is determined by cell division [14, 15]. The predominance of pentagons in marginal cells may also be explained by this model.

Discussion—We found that the average edge number \bar{n}_{MCs} of marginal cells in *P. haitanensis* thalli is approximately five, which is maintained by specific division patterns. We also proved that $\bar{n}_{MCs} = 5$ for 2D polygonal network with a coordination number strictly equal to three. By comparing the topological and geometrical parameters of marginal cells and inner cells, we observed significant limitations of Lewis's law and Aboav-Weaire's law. In addition, the specific topological feature of marginal cells changed the distributions of interior angles and edge lengths. From a methodological perspective, our results suggest that inner cells should be strictly defined based on their positional relationship to marginal cells, and that inner cells and marginal cells should be analyzed separately regarding cell proliferation, Lewis's law and Aboav-Weaire's law.

Acknowledgments—We thank Lingchao Zhang for his assistance on seaweed culture and image acquisition. KX acknowledges support from the National Natural Science Foundation of China (Grant No. 42376109).

References

- [1] WEAIRE D, RIVIER N. Soap, cells and statistics—random patterns in two dimensions [J]. Contemporary Physics, 1984, 25(1): 59-99.
- [2] CHIU S. Aboav-Weaire's and Lewis' laws—A review [J]. Materials Characterization, 1995, 34(2): 149-65.
- [3] ARAGON-CALVO M A. Scaling relations in the network of voids [J]. Monthly Notices of the Royal Astronomical Society: Letters, 2023, 522(1): L46-L50.
- [4] BÜCHNER C, HEYDE M. Two-dimensional silica opens new perspectives [J]. Progress in Surface Science, 2017, 92(4): 341-74.
- [5] CHERNOV N, HUANG Q, MA H. Fitting quadratic curves to data points [J]. British Journal of Mathematics & Computer Science, 2014, 4(1): 33-60.
- [6] SU H. The characteristics of maximum inscribed and minimum circumscribed polygons of ellipse [J]. Teaching Mathematics 1987, 6: 22-6.
- [7] XU K, XU Y, JI D, et al. Cells tile a flat plane by controlling geometries during morphogenesis of *Pyropia thalli* [J]. PeerJ, 2017, 5: e3314.
- [8] LEWIS F T. The effect of cell division on the shape and size of hexagonal cells [J]. The Anatomical Record, 1926, 33(5): 331-55.
- [9] LEWIS F T. The correlation between cell division and the shapes and sizes of prismatic cells in the epidermis of cucumis [J]. The anatomical record, 1928, 38(3): 341-76.
- [10] ABOAV D A. The arrangement of cells in a net. IV [J]. Metallography, 1985, 18(2): 129-47.
- [11] WEAIRE D. Some remarks on the arrangement of grains in a polycrystal [J]. Metallography, 1974, 7(2): 157-60.
- [12] XU K. A geometry-based relaxation algorithm for equilibrating a trivalent polygonal network in two dimensions and its implications [J]. Philosophical Magazine, 2021, 101(14): 1632-53.
- [13] XU K. Ellipse packing in two-dimensional cell tessellation: a theoretical explanation for Lewis's law and Aboav-Weaire's law [J]. PeerJ, 2019, 7: e6933.
- [14] GIBSON M C, PATEL A B, NAGPAL R, et al. The emergence of geometric order in proliferating metazoan epithelia [J]. Nature, 2006, 442(7106): 1038-41.
- [15] NAGPAL R, PATEL A, GIBSON M C. Epithelial topology [J]. BioEssays, 2008, 30(3): 260-6.
- [16] GIBSON W T, VELDHUIS J H, RUBINSTEIN B, et al. Control of the Mitotic Cleavage Plane by Local Epithelial Topology [J]. Cell, 2011, 144(3): 427-38.
- [17] VICENTE-MUNUERA P, GOMEZ-GALVEZ P, TETLEY R J, et al. EpiGraph: an open-source platform to quantify epithelial organization [J]. Bioinformatics, 2020, 36(4): 1314-6.

Fig. 1 Positions of MC, NC-MC, IC, MA, and ME in a *P. haitanensis* tissue (a). Distribution of n (b). Diagram shows the methods of proof for $\bar{n}_{MCs} = 5$ (c). Relationships between n and A_c (d), n and P (e), n and m (f). Numbers of examined cells are shown in parentheses.

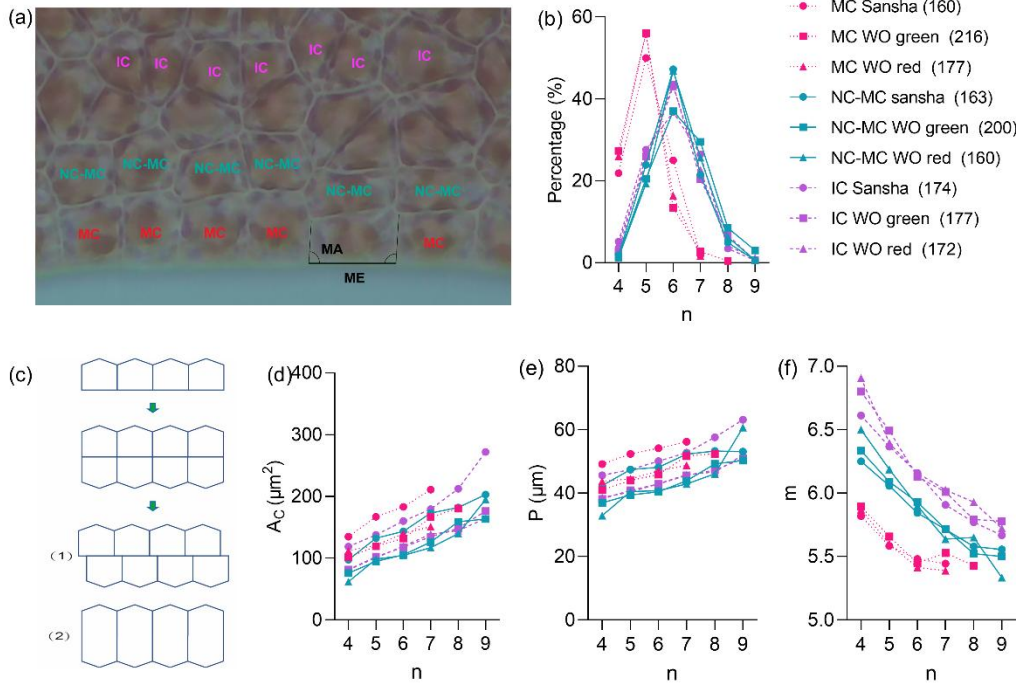


Fig. 2 Angles (a) and edge lengths (b) of cells from WO red. Sample numbers are shown in parentheses.

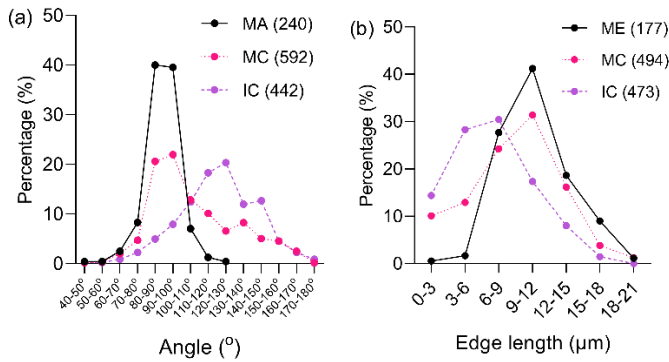


Fig. 3 Differences between resting cells and dividing cells in A_c (a), P (b), a/b , n , and m (c). For the latter three parameters, the data of all strains and mutants are combined. The numbers on bars denote the numbers of cells.

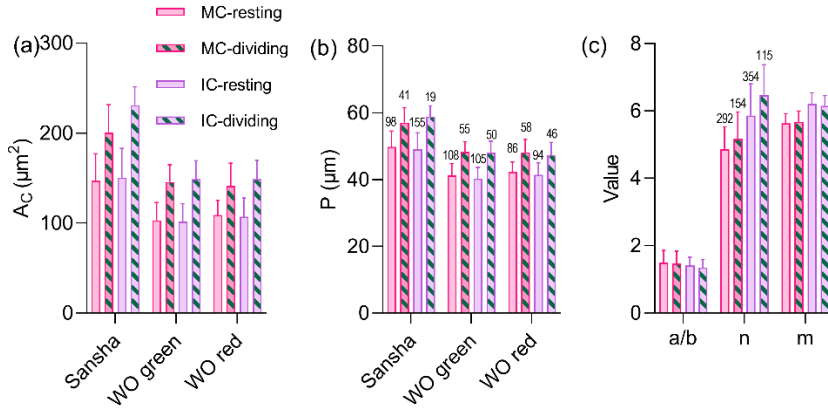
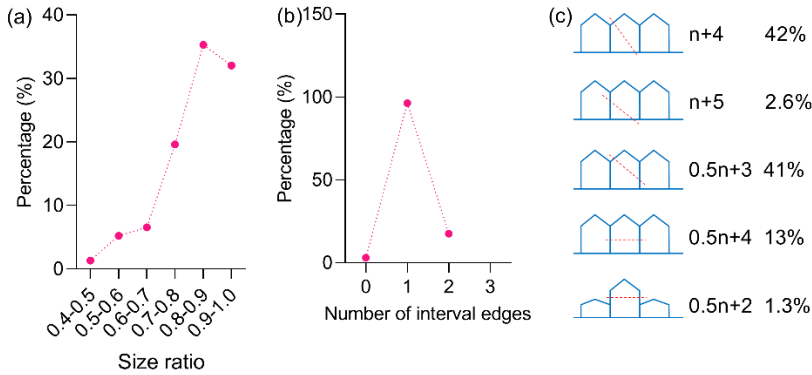


Fig. S1 Size ratio of daughter cells (a), smaller number of interval edges (b), and division patterns (c) of marginal cells (MCs). The division of n -edged MC changes the edge number of MCs. The final edge number (including changes on neighboring MCs to simplify the calculation) and the percentage of each type of division patterns are shown at the right side of (c). The number of examined dividing MCs were 153.



Tab. S1 Parameters of polygonal cells and fitted ellipses in *P. haitanensis*. Parameters n , m , A_C , P , a , b , and A_{EMIP} represent the edge number, average edge number of neighboring cells of an n -edged cell, area, perimeter, semi-major-axis, semi-minor-axis, and the area of the ellipse's maximal inscribed polygon, respectively.

Parameters	MCs			NC-MCs			ICs		
	Sansha	WO green	WO red	Sansha	WO green	WO red	Sansha	WO green	WO red
n	5.04±0.77	4.93±0.75	4.94±0.70	6.06±0.88	6.32±1.04	6.18±0.88	5.97±0.97	6.04±0.95	6.01±0.96
m	5.62±0.31	5.69±0.31	5.64±0.29	5.86±0.29	5.86±0.34	5.88±0.32	6.16±0.32	6.19±0.34	6.21±0.33
A_C (μm^2)	163.69±37.79	117.78±28.01	122.20±25.08	148.49±34.97	115.15±30.96	108.75±23.82	159.23±40.25	118.62±29.71	118.93±29.36
P (μm)	52.02±5.59	43.67±4.87	44.76±4.36	49.02±5.84	42.21±5.46	41.59±4.68	50.13±5.68	43.10±4.98	43.00±4.76
a (μm)	11.07±1.74	9.50±1.91	9.55±1.72	10.27±1.65	8.42±1.48	8.57±1.71	9.99±1.32	8.67±1.17	8.68±1.23
b (μm)	7.66±1.11	6.40±0.98	6.70±1.02	6.84±0.94	6.06±0.85	5.99±0.86	7.28±0.94	6.28±0.89	6.35±0.82
a/b	1.47±0.33	1.53±0.43	1.47±0.40	1.53±0.35	1.41±0.33	1.46±0.41	1.39±0.24	1.40±0.25	1.39±0.26
A_{EMIP} (μm^2)	200.48±54.29	141.40±39.55	148.28±37.23	181.28±41.31	134.22±34.77	133.59±34.72	187.05±44.03	140.96±34.43	141.83±33.57
A_C/A_{EMIP}	0.83±0.10	0.85±0.09	0.84±0.10	0.82±0.09	0.86±0.07	0.83±0.09	0.85±0.08	0.84±0.09	0.84±0.10